Anomalous charge oscillations in the dynamical response of metals

Kieron Burke* and W. L. Schaich
Department of Physics, Indiana University, Bloomington, Indiana 47405
(Received 9 December 1993)

In recent calculations of optical response at a metal surface, an unusual set of oscillations have been found in the induced charge density. These oscillations only appear when a crystal potential is included in the calculation. They propagate deep into the bulk, but are incommensurate with the lattice. We illustrate the occurrence of such oscillations in simple systems, and discuss their origin. For more general cases, we find that the amplitude of the oscillations is sensitive to the amount of spatial variation in directions parallel to the surface of either the crystal potential or the probing field. We also discuss the challenge of detecting this phenomenon experimentally.

I. INTRODUCTION

Considerable progress has been made toward understanding the long-wavelength response of the surfaces of nearly-free-electron metals (Na,K,Cs,Al).[1,2] This success has been possible because such metals are apparently well approximated by a semi-infinite slab of jellium. Early attempts in this field, using an infinite barrier at the surface, failed to explain several features, even qualitatively, e.g., the dispersion of the surface plasmon.[3] A major breakthrough occurred when Feibelman included a self-consistent surface barrier, and solved the resulting integral equations.[1] Since then, many refinements and more sophisticated calculations have yielded good agreement with experiment for these metals.[4] These advances include the identification of the so-called multipole mode, which was subsequently observed in electron energy loss experiments.[5]

The theory of surface response for metals with significant band structure is far less developed.[6] This is regrettable, as there is no experimental difficulty in investigating such surfaces, and several cases have already been studied.[7] In particular the effects observed in the surface plasmon dispersion on Ag surfaces[8] have stimulated various extensions of jellium treatments,[9] but these lack the rigor of the earlier jellium calculations for the free-electron like metals.

Another approach currently being pursued is to include the band structure in an *ab initio* fashion.[10–14] The drawback to this approach is the considerable numerical difficulty in solving the resulting integral equations. Once these difficulties have been overcome, such calculations should reveal new physics, and comparable agreement with experiment can be hoped for. An example of this appeared in recent calculations by Burke and Schaich[12] and by Samuelson and Schattke,[14] in which oscillations were found in the dynamic charge density induced by a long-wavelength perturbation. Within an undamped random-phase-approximation (RPA) treatment of the response, these oscillations continue into the bulk of the solid indefinitely, despite being incommensurate with the bulk lattice. We shall refer to them as SCO for "surface-correction oscillations."

The purpose of this paper is to illustrate how SCO can arise even in simple models of electronic structure. In Sec. II we examine the dynamical response of a semi-infinite gas of noninteracting electrons, treating the crystalline potential in separate model calculations as either weak or strong. In each case we find oscillations in the linearly induced density which extend into the bulk but are incommensurate with both the perturbing potential and the lattice. We discuss why such a response is allowed, in spite of the translational invariance of the bulk. For the strong-scattering case, which we treat with a tight-binding model, we show how the amplitude of the oscillations is enhanced if there are optical transitions between parallel bands. Finally in Sec. III we discuss the general occurrence and experimental implications of these oscillations.

II. DYNAMICAL RESPONSE OF NONINTERACTING ELECTRONS

In this section, we calculate the response of simple systems to an external perturbation. For the first, all the relevant response information can be found analytically. The purpose of these models is to demonstrate unambiguously that a system with a surface can produce a long-range incommensurate response to an external potential. We emphasize that these models are not an appropriate theory for the surface response in general, but are simply pedagogical tools to clarify the origin of the new oscillations.

A. Free electrons

Consider a finite density of *noninteracting* electrons in three-dimensional space, confined to $x > 0$ by an infinite barrier, but with no other potential. We use the notation that lower-case boldface indicates a three-dimensional vector, and upper-case boldface indicates a two-dimensional wave vector, parallel to the surface. Thus we write the position vector $\mathbf{x} = (x, \mathbf{X})$. Throughout this paper, $\hbar = 1$ and only the nonretarded limit is

considered. Note that all quantities in the dynamical response will have an $\exp(-i\omega t)$ time dependence, and depend on the particular frequency ω, but we do not write this dependence explicitly. As the particles are noninteracting, their linear response to an external potential is simply given by

$$\delta n(\mathbf{x}) = \int_{x'>0} d^3x' \chi_0(\mathbf{x},\mathbf{x}') V_{\rm ext}(\mathbf{x}'), \tag{1}$$

where $\delta n(\mathbf{x})$ is the induced density, $V_{\rm ext}(\mathbf{x}')$ is the external potential, and $\chi_0(\mathbf{x},\mathbf{x}')$ is the independent-particle susceptibility. This may be written quite generally as

$$\chi_0(\mathbf{x},\mathbf{x}') = 2\sum_{n,n'} \frac{f(\epsilon_n) - f(\epsilon_{n'})}{\epsilon_n + \omega - \epsilon_{n'}} \times \Psi_n^*(\mathbf{x})\Psi_{n'}(\mathbf{x})\Psi_{n'}^*(\mathbf{x}')\Psi_n(\mathbf{x}'), \tag{2}$$

where n labels the single-particle states of energy ϵ_n and wave function $\Psi_n(\mathbf{x})$. The function $f(\epsilon)$ is the Fermi occupation factor, which at zero temperature is just $\Theta(\epsilon_F - \epsilon)$, where $\Theta(u) = 1$ for $u > 0$, and zero otherwise, is the Heaviside step function. The factor of 2 comes from the sum over spin states.

Rather than analyze Eqs. (1) and (2) in real space,[14] we choose to work in Fourier space writing the transformed induced density in terms of the transformed external potential as

$$\delta n(q,\mathbf{Q}) = \int_0^\infty dq'\ \chi_0(q,q',\mathbf{Q})\ V_{\rm ext}(q',\mathbf{Q}), \tag{3}$$

where

$$\delta n(q,\mathbf{Q}) = \int_0^\infty dx \cos(qx) \int d^2X\ e^{-i\mathbf{Q}\cdot\mathbf{X}}\ \delta n(\mathbf{x}), \tag{4}$$

with a similar equation for $V_{\rm ext}(q,\mathbf{Q})$, and

$$\chi_0(q,q',\mathbf{Q}) = \frac{2}{\pi}\int_0^\infty dx \cos(qx) \int_0^\infty dx' \cos(q'x') \times \int d^2X\ e^{-i\mathbf{Q}\cdot(\mathbf{X}-\mathbf{X}')}\ \chi_0(\mathbf{x},\mathbf{x}'). \tag{5}$$

Note that we use regular Fourier transforms in the directions parallel to the surface but cosine Fourier transforms along the surface normal.

Equation (3) applies quite generally to systems which are uniform in directions parallel to the surface. For our simple model, the wave functions in the x direction are just $\Psi_n(x) = \sqrt{2}\sin(kx)$, and the usual plane waves in the parallel directions. Their energies are given by $\epsilon_{\mathbf{k}} = \mathbf{k}^2/2m$. We substitute these ingredients into the definition of the transformed susceptibility and, after writing sines and cosines as sums of plane waves, reduce the result to[12]

$$\chi_0(q,q',\mathbf{Q}) = \frac{2}{(2\pi)^3}\int_{\mathbf{K}'=\mathbf{K}+\mathbf{Q}} d^2K \int_{-\infty}^\infty \frac{dk}{2\pi}\int_{-\infty}^\infty \frac{dk'}{2\pi} \times \sum_{\sigma,\tau=\pm1} \sigma \frac{f(\epsilon_{\mathbf{k}}) - f(\epsilon_{\mathbf{k}'})}{\epsilon_{\mathbf{k}} + \omega - \epsilon_{\mathbf{k}'}} \times \langle k|\rho_q|k'\rangle\langle\sigma k'|\rho_{-\tau q'}|k\rangle, \tag{6}$$

where $\rho_q(x) = e^{-iqx}$ and the matrix elements are calculated with bulk states; e.g.,

$$\langle k|\rho_q|k'\rangle = \int_{-\infty}^\infty dx\ e^{-i(k+q-k')x} = 2\pi\delta(k+q-k'). \tag{7}$$

It is useful to view the susceptibility in (6) as the sum of two pieces, based on the sign of σ. We call these the direct and reflected contributions, writing

$$\chi_0(q,q',\mathbf{Q}) = \chi_0^{\rm dir}(q,q',\mathbf{Q}) + \chi_0^{\rm refl}(q,q',\mathbf{Q}) \tag{8}$$

and represent them with the scattering diagrams in Figs. 1(a) and 1(b), respectively, each to be summed over $\tau = \pm 1$. These pictures represent expressions based on *bulk* quantities, ranges, and rules.[15] The plain solid lines represent the bulk propagator

$$\tilde{G}(E) = \sum_{\mathbf{k}} \frac{|\mathbf{k}\rangle\langle\mathbf{k}|}{E - \epsilon_{\mathbf{k}} + i\delta_{\mathbf{k}}}, \tag{9}$$

where $|\mathbf{k}\rangle = |k,\mathbf{K}\rangle$ is a plane wave, and $\delta_{\mathbf{k}} = 0^+$ for $\epsilon_{\mathbf{k}} > \epsilon_F$, and $\delta_{\mathbf{k}} = 0^-$ for $\epsilon_{\mathbf{k}} < \epsilon_F$. The solid line with an X in the middle represents propagation in which a reflection off the barrier occurs

$$\tilde{G}_X(E) = -\sum_{\mathbf{k}} \frac{|k,\mathbf{K}\rangle\langle -k,\mathbf{K}|}{E - \epsilon_{\mathbf{k}} + i\delta_{\mathbf{k}}}. \tag{10}$$

The extra minus signs are necessary to produce the $\sigma = -1$ term of (6). They arise because the true eigenstates of the surface problem are sine waves, not plane waves.

The direct contribution has terms proportional to $\delta(\tau q' - q)$ and, since q, q' are positive, only the $\tau = 1$ piece is nonzero. In fact

$$\chi_0^{\rm dir}(q,q',\mathbf{Q}) = \chi_0^B(\mathbf{q})\delta(q-q'), \tag{11}$$

where $\mathbf{q} = (q,\mathbf{Q})$ and $\chi_0^B(\mathbf{q})$ is the susceptibility of the bulk system, Fourier transformed in all three directions.

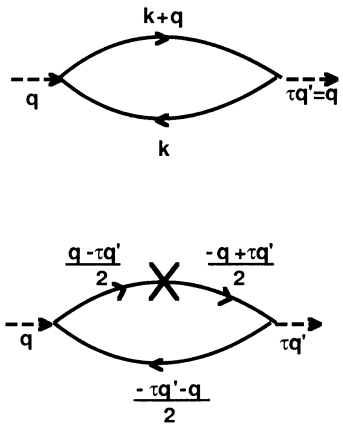

FIG. 1. Scattering diagrams representing the two contributions to the susceptibility of free electrons near a surface. The dashed lines represent the external momenta, while the solid lines are particle (or hole) propagators. The X on the particle propagator in (b) indicates that it includes a surface reflection.

For the free electrons discussed here, $\chi_0^B(\mathbf{q})$ is given by the Lindhard function.[15]

The reflected contribution is due to the presence of the surface. In physical terms, if we imagine the perturbation virtually exciting a particle-hole pair, then it is possible for one member of the pair to be reflected off the surface before the two recombine. This reflection is described by the momentum-reversal propagator for the particle line in Fig. 1(b). The reflection reverses the particle's momentum normal to the surface, thereby destroying the translational invariance of the scattering process. Hence such contributions are not proportional to $\delta(q-\tau q')$, and in fact are relatively smooth functions of q and q'. However their integrated weights in (3) are typically comparable to that of $\chi_0^{\rm dir}$. Note that, in terms of the diagrams of Fig. 1, momentum conservation at each vertex and the sum on $\tau = \pm 1$ guarantee that we have found all the independent contributions. If for instance one were to reverse all the normal momenta at the right vertex in Fig. 1(b) and simultaneously change τ to $-\tau$, it would not affect the numerical value of the diagram, but the anomalous propagator would then appear (only) for the hole line.

It is straightforward to evaluate the reflected contribution for $\mathbf{Q} = \mathbf{0}$. In that case, the integrand becomes independent of $\mathbf{K}$, except in the Fermi factor cutoff, and

$$\int d^2K f(\epsilon_{\mathbf{k}}) = 2\pi m \Phi(\epsilon_F - \epsilon_k), \tag{12}$$

where $\Phi(u) = u\Theta(u)$. Furthermore, because of the breaking of translational symmetry, the δ functions due to the two vertices serve to remove the two integrals over normal momentum. The result is simply[16]

$$\chi_0^{\rm refl}(q,q') = \frac{1}{4\pi^2}\frac{qq'}{\omega^2 - (qq'/2m)^2} \times \sum_{\tau=\pm 1} \tau \Phi\left(\epsilon_F - \epsilon_{\frac{q+\tau q'}{2}}\right). \tag{13}$$

Now we are ready to demonstrate how the presence of the reflected contribution in χ_0 can produce an unusual oscillation in the density response. Imagine perturbing these particles with an external potential of the form

$$V_{\rm ext}(x,t) = \cos(g_0 x) e^{-i\omega t}. \tag{14}$$

(In Sec. III we describe how such a perturbation can arise in the full crystal problem.) The cosine transform of the perturbation produces a δ function in q space, which leads to a density response in real space of

$$\delta n(x) = \chi_0^B(g_0)\cos(g_0 x) + \int_0^\infty dq \cos(qx)\chi_0^{\rm refl}(q,g_0). \tag{15}$$

For simplicity, we look at just the imaginary part of this response. Then the integral over q in the reflected term becomes trivial, as the energy denominator in (13) just yields a δ function, i.e.,

$$\mathrm{Im}\left[\chi_0^{\rm refl}(q,q',\omega)\right] = -A(q',\omega)\delta(q - 2m\omega/q'), \tag{16}$$

where Im means "imaginary part of" and

$$A(q',\omega) = \frac{m^2}{2\pi q'}\sum_{\tau=\pm 1}\tau\Phi\left(\frac{k_F^2}{2m} - \frac{[2m\omega/q' + \tau q']^2}{8m}\right). \tag{17}$$

We find

$$\mathrm{Im}[\delta n(x)] = A(g_0,\omega)[\cos(g_0 x) - \cos(q_1 x)], \tag{18}$$

where $q_1 = 2m\omega/g_0$. The coefficient $A(q,\omega)$ is also equal to the imaginary part of the Lindhard function in (11),[15] evaluated at q and ω. This surprisingly simple result is dictated by the requirement that $\delta n(x)$ must vanish at $x = 0$, due to the infinite barrier. Much more remarkable is the fact that a second oscillation has developed, which in general is incommensurate with the first, and which continues indefinitely into the interior.

How can this system support an oscillation at a different wavelength from that of the driving potential far from the surface? Should it not be forbidden by translational invariance? The answers to these objections can be found in two general features of the calculation. The first is the fact that, even far from the surface, the single-particle eigenstates are generally coherent sums of Bloch states. For our free-electron model with an infinite barrier, this merely means that $\Psi_n(x) = \sqrt{2}\sin(kx)$ rather than e^{ikx}. For *equilibrium* properties, this coherence is unimportant far from the surface. For example, consider the calculation of the equilibrium density,

$$n_0(x) = \frac{2}{(2\pi)^2}\int d^2K \frac{2}{\pi}\int_0^\infty dk\, f_{\mathbf{k}} \sin^2(kx) = \frac{m}{\pi^2}\int_0^{k_F} dk\, \Phi(\epsilon_F - \epsilon_k)\,[1 - \cos(2kx)]. \tag{19}$$

The constant term in the integrand leads to the bulk value $n_0^B = \frac{k_F^3}{3\pi^2}$, while the oscillating corrections die away within a few k_F^{-1} due to phase cancellations in the integral. Thus $n_0(x)$ quickly returns to its bulk value. If, however, one looks at a single k value, the oscillating terms survive for all x.

This brings us to the second general feature. In the dynamic response there are energy-conserving transitions for which (bulk) momentum conservation restricts the sum over contributing states so that "surface corrections" can remain in phase for large distances. In terms of our free-electron model we need to satisfy $\epsilon_k + \omega = \epsilon_{k'}$ with $k' = k + g_0$. Eliminating k' yields $k = \frac{m\omega}{g_0} - \frac{g_0}{2} = \frac{q_1 - g_0}{2}$. Hence $k' + k = 2k + g_0 = q_1$ and $k' - k = g_0$ so the induced density, which in linear response is determined by the cross product of initial and final states, becomes proportional to

$$2\sin kx\, \sin k'x = \cos(k - k')x - \cos(k + k')x = \cos(g_0 x) - \cos(q_1 x). \tag{20}$$

The spatial dependence of (20) reproduces that of (18). Each pair of states that contributes to $\delta n(x)$ through an energy- and (bulk) momentum conserving process produces the same x dependence. Different such pairs only

differ in parallel momenta and one simply integrates over $\mathbf{K}$ to find their overall contribution. Hence the x dependence of the SCO is not washed out [as it is in $n_0(x)$] by the integral over contributing states.

Why have these long-ranged SCO not appeared in earlier calculations of bulk response? The simple answer is that the phase coherence of the eigenstates necessary for the existence of the SCO is ignored in typical "bulk" calculations.[15] For instance, consider the response of our model system if we impose periodic boundary conditions at the edges in x, instead of requiring the wave function to vanish at these points. Then the eigenstates are plane waves, the susceptibility is determined by $\chi_0^B(\mathbf{q})$ alone, and the response $\delta n(x)$ contains only the commensurate oscillation. Given that the SCO of (18) continue indefinitely into the interior of the system, it would appear that the response in the bulk depends on the boundary conditions at (distant) surfaces. A resolution of this ambiguity can be found in the fact that the single-particle states in physical systems must have a finite lifetime (or equivalently, a finite range of coherence), as discussed in Sec. III. The effect of such a lifetime can be simulated by giving ω in (13) a small but finite imaginary piece, so that the pole in the energy denominator is moved slightly off the real axis, producing a slow but finite decay to the incommensurate contribution in (18). Thus, far from the surface the SCO become negligible and one is left with the conventional bulk response, which can be correctly calculated using plane waves.

B. Tightly bound electrons

Next we turn to a tight-binding model of electronic structure, which is at the opposite extreme from free electrons. We still assume independent particles so the analysis is again based on Eqs. (1) and (2), but the eigenstates and energies will have a different form. We use as a basis set for the electrons well localized orbitals centered on the Bravais lattice points of the (100) face of a semi-infinite simple cubic lattice and ignore all overlaps between neighbors, except for nearest-neighbor hopping integrals between like orbitals. The parameters are chosen so the partially occupied lowest band is built from s-wave orbitals, while the three (degenerate) unoccupied bands use p-wave orbitals. For an applied field normal to the surface, only transitions to one of these bands are allowed, so we have in effect a two-band model of optical excitations. Although we place the Fermi level within the lowest band (and completely below the upper bands), we shall ignore all intraband excitations. With these simplifications we can produce a fairly explicit solution. The eigenstates are written as

$$\Psi_{\mathbf{k}\alpha}(\mathbf{r}) = \frac{1}{\sqrt{N_s}} \sum_l e^{i\mathbf{K}\cdot\mathbf{R_L}}\, b_{kl\alpha}\, \varphi_\alpha(\mathbf{r}-\mathbf{r}_l), \tag{21}$$

with eigenenergy

$$\epsilon_{\mathbf{k}\alpha} = \epsilon_\alpha + \sum_{\mathbf{m}} \Delta_{\mathbf{m}\alpha}\, e^{i\mathbf{k}\cdot\mathbf{r}_\mathbf{m}}. \tag{22}$$

Here the lattice sites are labeled by the vector index l and the sum in (22) runs over nearest neighbors of any site, while in (21) N_s is the (macroscopic) number of sites within a plane parallel to the surface. The orbitals are real-valued functions and we denote by φ_0 the s-wave orbital and by φ_1 the p-wave orbital with the symmetry of x. Our neglect of overlaps between neighbors lets us write

$$\int d^3r\, \varphi_\alpha(\mathbf{r}-\mathbf{r}_l)\, \varphi_{\alpha'}(\mathbf{r}-\mathbf{r}_{l'}) = \delta_{\alpha,\alpha'}\delta_{l,l'}. \tag{23}$$

The orbital eigenvalue of φ_α is ϵ_α and the $\Delta_{\mathbf{m}\alpha}$ are the overlap integrals with the Hamiltonian between like orbitals on adjacent sites. The $b_{kl\alpha}$ are dimensionless weights, which from orthonormality of the eigenstates obey

$$\sum_l b^*_{k'l\alpha'}\, b_{kl\alpha} = \delta_{k',k}, \tag{24}$$

for any combination of α and α'.

To avoid needing to specify the detailed form of the φ_α we focus on calculating the induced dipole moment at each site due to interband transitions driven by a spatially uniform field along x. The relevant moments are defined by

$$p_{01}(l) = \int_{\mathbf{r}\ \text{near site}\ l} d^3r e\mathbf{r}\, \delta n_{01}(\mathbf{r}). \tag{25}$$

The δn_{01} required in (25) is defined by retaining in (1,2) only the contributions due to 0–1 interband transitions.[17] For a uniform driving field $\mathbf{E}$ along x we find

$$p_{01}(l) = \frac{2}{N_s} \sum_{\mathbf{k}} f(\epsilon_{\mathbf{k}0})\, \frac{2(\epsilon_{\mathbf{k}0}-\epsilon_{\mathbf{k}1})}{(\epsilon_{\mathbf{k}0}-\epsilon_{\mathbf{k}1})^2-\omega^2}\, b^*_{kl0}\, b_{kl1}\, DE, \tag{26}$$

where D is defined by dipole matrix element at a single site:

$$D = e^2\langle\varphi_1|x|\varphi_0\rangle^2. \tag{27}$$

Since the on-site energies and hopping integrals do not depend on l, the spatial dependence of the b's in either band is proportional to $\sin(kla)$ where a is the lattice constant. In the continuum limit

$$b^*_{kl0}b_{kl1} = 2\sin^2(kla) = 1-\cos(2kla), \tag{28}$$

which when summed over $\mathbf{k}$ in (26) will produce both the expected uniform response plus an oscillatory piece whose period and range depend on the variation with $\mathbf{k}$ of the other factors in (26). Unlike in the free-electron model, we cannot do the integrals analytically but they are readily evaluated numerically and we have the freedom of adjusting the relative shape of the contributing bands. If we choose parameters so the two bands are parallel as a function of $\mathbf{K}$, then $\epsilon_{\mathbf{k}0}-\epsilon_{\mathbf{k}1}$ is independent of $\mathbf{K}$ and the integrand in (26) will have an (isolated) pole contribution from the plane inside the Fermi surface

where $\epsilon_{\bar{k},\mathbf{K}0} + \omega = \epsilon_{\bar{k},\mathbf{K}1}$. This will produce a piece of $p_{01}(l)$ oscillating at $\bar{k}$ deep into the bulk, which is the tight-binding version of the SCO.

We can also examine how robust the anomaly is as the bands are allowed to become nonparallel. We do this from the cosine Fourier transform of p_{01}, which away from $q = 0$ is given by

$$p_{01}(q) = -\frac{a^2}{4\pi^2}\int d^2K\, f(\epsilon_{q/2,\mathbf{K}0}) \times \frac{(\epsilon_{q/2,\mathbf{K}0} - \epsilon_{q/2,\mathbf{K}1})}{(\epsilon_{q/2,\mathbf{K}0} - \epsilon_{q/2,\mathbf{K}1})^2 - (\omega + i\gamma)^2}, \quad (29)$$

where to ease the numerical evaluation we have added a broadening by replacing $\omega \to \omega + i\gamma$. Our specific parameter choices yield

$$\epsilon_0/v = 6 - 2[\cos k_x a + \cos k_y a + \cos k_z a], \quad (30)$$

$$\epsilon_1/v = 15 + 4(\lambda - 1) + 6\cos k_x a - 2\lambda[\cos k_y a + \cos k_z a], \quad (31)$$

where v sets the energy scale and λ controls how similar the upper band is in its $\mathbf{K}$ variation to the lower band. For $\lambda = 1$, the two bands are parallel as a function of $\mathbf{K}$. Note that λ also appears in the offset of the upper band to insure that the separation between the bands is independent of λ for $\mathbf{K} = \mathbf{0}$ as shown in Fig. 2(a). The λ dependence of the upper band is only evident for $\mathbf{K} \neq \mathbf{0}$, and is illustrated in Fig. 2(b). In Fig. 2(c) we show how the sharp peak in $p_{01}(q)$ for parallel bands (when $\lambda = 1$) spreads (and shifts) for $\lambda \neq 1$, describing the nonparallel bands of Fig. 2(b). For the range of λ used, the broadening of the peak in the transform (and hence the decay in real space of the SCO) is not extreme. Furthermore, the integrated weights of the structures in Fig. 2(c) vary slowly with λ. Hence the anomalous oscillations do not quickly disappear for slight deviations from parallel bands. However they do decrease in strength and range and eventually become negligible. In Ref. 17 their presence was formally suppressed, in part because the upper band was much flatter and the analog of the λ parameter used here was 1/4 so the transform of p_{01} is spread over about half a zone.

Having just shown how the SCO can be reduced by allowing for variations in the crystal potential in directions parallel to the surface (which is the basic cause of nonparallel bands), it is appropriate to return to the free-electron calculation and examine how the SCO behave there when one allows the probe field to vary with $\mathbf{X}$. Specifically we replace (14) with

$$V_{\text{ext}}(\mathbf{x}, t) = e^{i\mathbf{Q}\cdot\mathbf{X}}\cos(g_0 x)\, e^{-i\omega t} \quad (32)$$

and consider how $\delta n(x, \mathbf{Q})$ changes as $Q = |\mathbf{Q}|$ is increased. In physical terms, such $\mathbf{X}$ variations of the probe field are easily produced in electron scattering experiments and the mapping of an excitation's dispersion with $\mathbf{Q}$ and ω is a standard procedure. At finite $\mathbf{Q}$ the susceptibility can still be found analytically and for the reflected piece we obtain

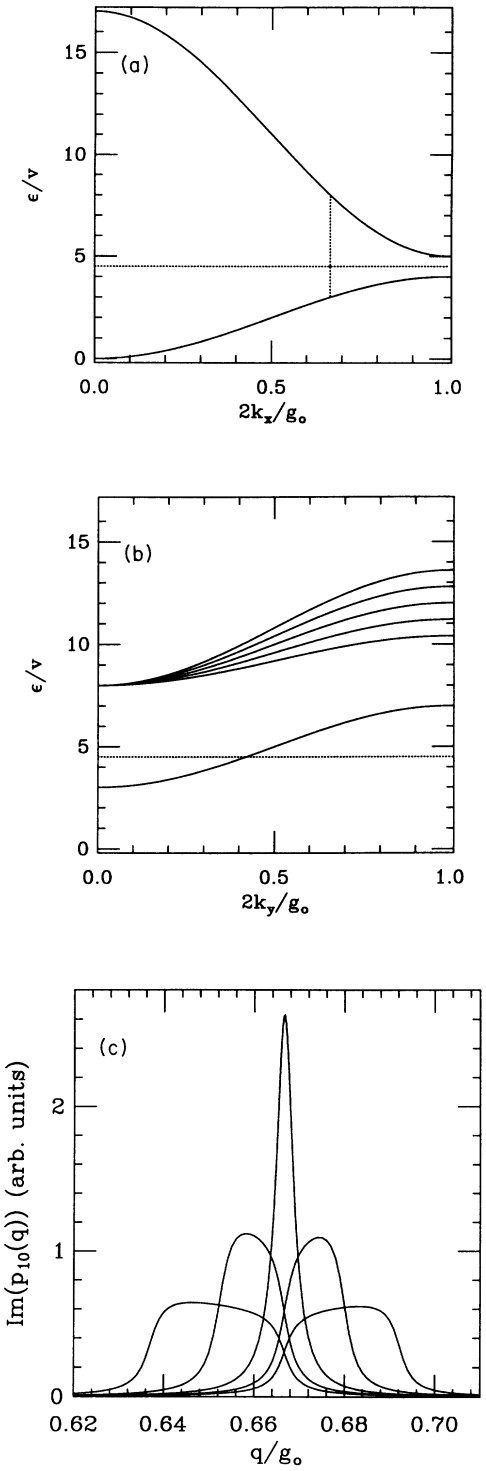

FIG. 2. In (a) and (b) the band structure of the two-band, tight-binding model is shown in different directions. In (a) $\mathbf{K} = \mathbf{0}$ while in (b) $k_x = \bar{k}$ and $k_z = 0$. The horizontal dashed line is the Fermi level and the vertical dashed line in (a) locates the direct transition for $\omega/v = 5, \mathbf{K} = \mathbf{0}$. The family of upper-band curves in (b) is produced by different values of λ running from 0.6 to 1.4 in steps of 0.2 as the curves move from lower to higher energies. The same set of λ determines the plots of the imaginary part of the cosine Fourier transform of p_{01} shown in (c) for $\omega/v = 5$. As λ grows the center of the transform moves to larger q.

$$\mathrm{Im}[\chi_0^{\mathrm{refl}}(q,g_0,\mathbf{Q})] = \frac{m}{4\pi^2 Q}\sum_{\sigma,\tau=\pm 1}\sigma\Phi\left(\sqrt{(k_F^o)^2-\left(\frac{q+\tau g_0}{2}\right)^2}-\left(\frac{\tau q g_0+2m\sigma\omega-Q^2}{2Q}\right)^2\right), \tag{33}$$

where k_F^0 is the Fermi wave vector. The variation with q of (33) describes how the SCO become spread out over a range of wave vectors because at finite $\mathbf{Q}$ the difference in "parallel" energies of an electron-hole pair, $(2\mathbf{K}\cdot\mathbf{Q}+Q^2)/2m$, depends on $\mathbf{K}$. Typical results are shown in Fig. 3, using parameters appropriate to a free-electron model of Li with $r_s = 3.26$. The driving frequency is 1.3 times the Fermi energy, $g_0 = 2\pi/a$ with $a = 2.48$ Å the spacing between planes in the (110) direction, and we plot for $Q/g_0 = 0.05, 0.15, 0.25, 0.35, 0.45$ to produce curves of increasing diffuseness and/or decreasing strength. For $Q/g_0 > 0.467$ it is no longer possible to satisfy energy and momentum conservation in transitions from initial states below the Fermi level and the SCO completely disappear. Hence, as with nonparallel bands, variations in $\mathbf{X}$ of the probe field act to suppress the SCO.

III. GENERALIZATIONS AND EXPERIMENTAL CONSEQUENCES

By studying simple models in the previous section we were able to make considerable analytic progress. However the results obtained are at best only qualitative. For a quantitatively reliable theory much more must be included. We now discuss these required improvements under the two general headings of (i) a self-consistent treatment of many-body interactions and (ii) a better treatment of one-body effects.

At a mean-field level, which is the usual approximation, the necessary changes in Eqs. (1) and (2) are formally slight. The external potential is augmented by an induced potential to create an effective potential to which the individual particles respond:

$$\delta n(\mathbf{x}) = \int_{x'>0} d^3x'\,\chi_0(\mathbf{x},\mathbf{x}')\,V_{\mathrm{eff}}(\mathbf{x}'), \tag{34}$$

where $V_{\mathrm{eff}} = V_{\mathrm{ext}} + V_{\mathrm{ind}}$ with

$$V_{\mathrm{ind}}(\mathbf{x}') = \int d^3x''\,v(\mathbf{x}'-\mathbf{x}'')\,\delta n(\mathbf{x}'') + \cdots, \tag{35}$$

and $v(\mathbf{x}) = e^2/|\mathbf{x}|$. In (35) we have only explicitly shown the Hartree contribution due to the Coulomb potential of the total density fluctuation, δn. This is all that is kept in the random-phase approximation of the response. One often goes further to include in (35) a local density functional expression for the induced changes in the exchange and correlation potentials. We only stress here that (34, 35) must be solved self-consistently for δn.

The perturbation (14) that we used to perturb free electrons in Sec. II can be viewed as really arising from V_{ind} due to the periodic variation of δn in the bulk of the crystal. Thus a bulk umklapp process can create from a long-wavelength perturbation a periodic contribution to δn with wave vector g_0 along x, whose induced potential creates via equations like (18) contributions at both g_0 and q_1 to δn, and so on. Such effects are visible in Ref. 12, where they are discussed in detail. One ends up with a whole collection of special wave vectors related by sequences of energy-conserving scattering events of bulk umklapp processes and surface reflections.

The self-consistent calculation of the amplitudes of these oscillations is a difficult numerical task even for simple models of the one-body potential. However, the screening processes represented by such solutions cannot eliminate the SCO. To exhibit some typical results we show in Fig. 4 the imaginary part of the induced density profile from a dynamical response calculation. The computation was done as described elsewhere,[12] with parameters chosen to model the Li(110) optical response. It was performed within the RPA, using an infinite barrier at the surface, an effective mass, and a one-dimensional lattice with a single Fourier component of potential energy:

$$V(\mathbf{x}) = 2V_0\cos(g_0 x). \tag{36}$$

The frequency of the perturbation is $1.3\epsilon_F^0$, where ϵ_F^0 is the free-electron Fermi energy. This frequency is below the bulk plasmon band which starts at $1.6\epsilon_F^0$ but above both the interband threshold at $0.6\epsilon_F^0$ and the zone-boundary collective states which end at $1.1\epsilon_F^0$. We have plotted in addition to $\mathrm{Im}[\delta n]$ the separate bulk and surface-correction pieces. The former is determined by[11]

$$4\pi\delta n^B(x) = -\sum_g \epsilon^{-1}(g,0)g\sin(gx)\;E, \tag{37}$$

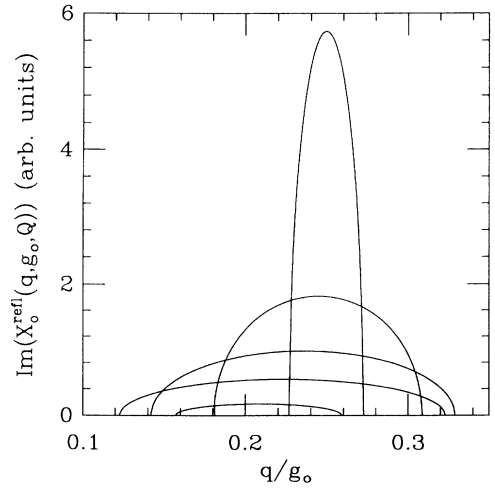

FIG. 3. Imaginary part of the reflected contribution to the free-particle susceptibility for Q/g_0 =0.05, 0.15, 0.25, 0.35, 0.45, for the highest to the lowest peak, respectively. This function becomes proportional to a δ function at $q_1 = 0.25g_0$ as $Q \to 0$.

where E is the (constant) value of the electric field along x outside the metal, the $\epsilon^{-1}(g,0)$ are elements of the inverse dielectric matrix of the bulk, and the sum on g runs over integral multiples of g_0. Subtracting δn^B in the middle plot from δn in the bottom plot gives the SCO shown in the top plot. The cosine Fourier transform of the SCO has sharp peaks at two wave vectors: $0.24g_0$ and $0.76g_0$ which, in the notation of the free electron model, we should identify as q_1 and $g_0 - q_1$. The free-electron formula for q_1 is $\frac{2m\omega}{g_0}$, which predicts $q_1/g_0 = 0.25$, remarkably close given that it ignores the distortion of the bands away from free-electron dispersion.

The incommensurate oscillations in Fig. 4 decay as one moves away from the surface. This has been forced to happen since we replaced $\omega \to \omega + i\gamma$ with $\gamma/\epsilon_F^0 = 0.025$ in the calculation. Larger values of γ make the SCO decay more quickly and the present code becomes too slow for smaller γ. From the simple models of the previous section we believe that the SCO would continue indefinitely if γ were zero. However, unavoidable incoherent scattering in real samples implies that γ should be nonzero. In addition higher-order many-body effects which act to blur the quasiparticle concept by mixing various single-particle states together will also cause the eventual decay of the SCO. Still, the important point is that the SCO extend significantly farther than a few lattice constants.

Now consider a better treatment of one-body effects. The recent numerical work[12,14] has used models in which crystallinity effects are allowed only as a function of x, the systems being uniform in $\mathbf{X}$. The bands are more complicated than in our free-electron or tight-binding models, but have the important simplification that they are all parallel in their dependence on $\mathbf{K}$. It is then straightforward to rationalize the appearance of SCO in these calculations. The key is the continued presence of the two basic features responsible for SCO. The first is that integrating Schrodinger's equation through the surface can lead to an eigenstate becoming a linear combination

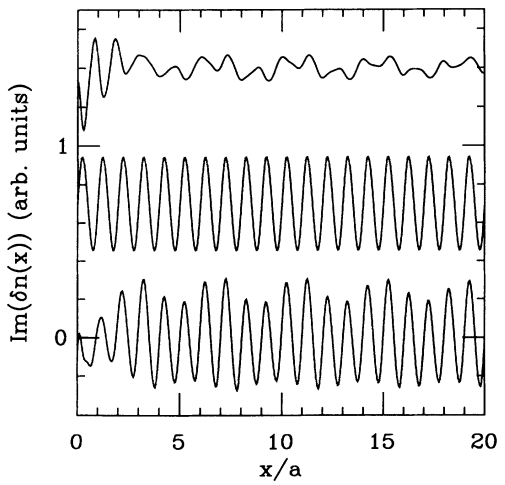

FIG. 4. Induced density response in a more sophisticated calculation (see text). The lowest curve is the total induced density while the upper two separate it into a bulk, periodic piece and the surface-correction oscillations. The curves have been offset for clarity.

of traveling Bloch waves in bulk. Although this is not always true for states above the vacuum level, it must occur for the occupied eigenstates. The second feature is that the constraint that optical transitions conserve energy and (some) bulk momentum leads to a restricted set of particle-hole pairs whose contributions to the density fluctuations do not cancel out as one moves into the bulk. What we mean by the adjective "some" here is the following. The eigenstates by the first feature do not in general have a unique crystal momentum in bulk, but instead are a linear combination of states that do. If the crystal momentum of a Bloch wave in the initial state matches the crystal momentum of a Bloch wave in the final state, we say that "some" bulk momentum has been conserved in the transition between the two states. For models of one-dimensional crystallinity the energy and bulk momentum constraints require in an extended zone scheme the simultaneous solution of $\epsilon_k + \omega = \epsilon_{k'}$ with $k = k'$, modulo g_0. At a fixed ω, these can be solved by only a few (k,k') pairs, usually one or zero. The surface corrections to the induced density due to all such pairs have the same form for all $\mathbf{K}$, and should produce long-ranged SCO.

When we try to move beyond one-dimensional models of crystallinity, the above argument breaks down because the "allowed" values of (k,k') will depend on $\mathbf{K}$ (and $\mathbf{K}'$) if the bands are not parallel. However, as we saw with the tight-binding model calculations, the existence question for SCO then becomes a difficult quantitative problem of amplitudes and ranges. It is probably best not to predict, but only to wait until such calculations are done.

Alternatively one could look to experiment for evidence of SCO. This too appears to be difficult. The problem is that the SCO are surface *corrections*. The separations of, say, χ_0 in Eq. (8) or δn in Fig. 4 are merely heuristic, since an experiment would probe the full χ_0 and δn. The SCO do not exist independently of interband transitions, unlike the various plasmons that can be excited at a surface. Thus even if one were to measure the reflection amplitude of either photons or electrons over an extended range of frequency, the SCO can only modify the spectral structure due to interband transition; i.e., once the interband transition threshold is crossed, the SCO also exist and how much they distort the spectrum is a question of matrix elements rather than density of states. For instance the frequency variation of $d_\perp$ calculated in Ref. 12 shows several sharp features attributed to SCO effects, but in fact the SCO are present throughout the interband range with roughly constant amplitude [with respect to the bulk oscillations of (37)] and range. There is no simple test to distinguish structure in the energy absorption by interband transitions as due to bulk matrix elements, SCO, or surface-localized modifications.

A more direct probe of the SCO is needed. One possibility that may be helpful is the study of nonlinear optics, where products of first-order local fields act as driving terms of higher-order processes.[18] We have in mind work along the lines of that by Song *et al.*[19] in which the dependence of second harmonic generation from Rb layers of varying thicknesses on Ag substrates was examined. Extracting clear evidence of the SCO will not be easy

because of a variety of competing effects, but one should at least do the analysis with their possible existence and long range in mind.

We conclude by mentioning that, although we have directed this discussion toward crystalline metal surfaces, SCO are generic features of the dynamical response of any system with a surface and a potential periodic in the direction perpendicular to that surface. Thus they should also occur in superlattices[20] and in periodically modulated quantum wells.[21] In fact, in such systems, the length scales associated with the lattice can be very different from those associated with the electron gas (in some cases, even adjustable), making them perhaps better candidates for detecting SCO than metals. Furthermore, these systems are constructed to make the gas as uniform as possible in the parallel direction. Therefore the bands should be very nearly parallel, producing a strong oscillation.

ACKNOWLEDGMENTS

We thank Kieran Mullen and Steve Girvin for helpful discussions. This work was supported in part by the National Science Foundation under Grant No. DMR-89-03851. Some of the calculations were done on the Cray Research, Inc., Y-MP4/464 system at the National Center for Supercomputing Applications at the University of Illinois at Urbana-Champaign (Champaign, IL).

* Present address: Department of Physics, Tulane University, New Orleans, LA 70118.

[1] P. J. Feibelman, Prog. Surf. Sci. **12**, 287 (1982).

[2] See, for example, W. L. Schaich and K. Kempa, Phys. Scr. **35**, 204 (1987); A. Leibsch, *ibid.* **35**, 354 (1987); A. G. Eguiluz, *ibid.* **36**, 651 (1987).

[3] For a good discussion, see, for example, R. R. Gerhardts, Phys. Scr. **28**, 235 (1983), and references cited therein.

[4] A. Leibsch, Phys. Rev. B **36**, 7378 (1987); K. Kempa, A. Liebsch, and W. L. Schaich, *ibid.* **38**, 12645 (1988); P. J. Feibelman, *ibid.* **40** 2752 (1989); P. J. Feibelman and K. D. Tsuei, *ibid.* **41** 8519 (1990).

[5] A. Eguiluz and J. J. Quinn, Phys. Lett. A **53**, 151 (1973); K.-D. Tsuei, E. W. Plummer, A. Liebsch, K. Kempa, and P. Bakshi, Phys. Rev. Lett. **64**, 44 (1990); K. D. Tsuei, E. W. Plummer, A. Liebsch, E. Pehlke, K. Kempa, and P. Bakshi, Surf. Sci. **247**, 302 (1991).

[6] E. W. Plummer, G. M. Watson, and K.-D. Tsuei, in *Surface Science*, edited by F. A. Ponce and M. Cardona, Springer Proceedings in Physics Vol. 62 (Springer-Verlag, Berlin, 1992).

[7] P. T. Sprunger, G. M. Watson, and E. W. Plummer, Surf. Sci. **269/270**, 551 (1992).

[8] S. Suto, K.-D. Tseui, E. W. Plummer, and E. Burstein, Phys. Rev. Lett. **63** 2590 (1989); M. Rocca and U. Valbusa, *ibid.* **64**, 2398 (1990); M. Rocca, M. Lazzarino, and U. Valbusa, *ibid.* **67**, 3197 (1991); G. Lee, P. T. Sprunger, E. W. Plummer, and S. Suto, *ibid.* **67**, 3198 (1991); M. Rocca, M. Lazzarino, and U. Valbusa, *ibid.* **69**, 2122 (1992); G. Lee, P. T. Sprunger, and E. W. Plummer, Surf. Sci. **286**, L547 (1993).

[9] J. Tarriba and W. L. Mochan, Phys. Rev. B **46**, 12902 (1992); P. J. Feibelman, Surf. Sci. **282**, 129 (1993); A. Leibsch, Phys. Rev. Lett. **71**, 145 (1993); A. Leibsch, Phys. Rev. B. **48**, 11317 (1993); E. Lipparini and F. Pederiva, Z. Phys. D **27**, 281 (1993).

[10] W. L. Schaich and W. Chen, Phys. Rev. B **39**, 10714 (1989).

[11] J.-T. Lee and W. L. Schaich, Phys. Rev. B **43**, 4629 (1991).

[12] K. Burke and W. L. Schaich, Phys. Rev. B **48**, 14599 (1993).

[13] D. Samuelson, A. Yang, and W. Schattke, Surf. Sci. **287/288**, 676 (1993).

[14] D. Samuelson and W. Schattke (unpublished).

[15] G. D. Mahan, *Many Particle Physics* (Plenum, New York, 1981).

[16] These expressions are well known, see, e.g., R. R. Gerhardts and K. Kempa, Phys. Rev. B **30**, 5704 (1984).

[17] W. L. Schaich, Phys. Rev. B **47**, 10852 (1993).

[18] A. Liebsch and W. L. Schaich, Phys. Rev. B **40**, 5401 (1989).

[19] K. J. Song, D. Heskett, H. L. Dai, A. Liebsch, and W. E. Plummer, Phys. Rev. Lett. **61**, 1380 (1988).

[20] J. Zhang, S. E. Ulloa; W. L. Schaich, Phys. Rev. B **41**, 5467 (1990); **43**, 9685 (1991).

[21] P. R. Pinsukanjana *et al.*, Phys. Rev. B **46**, 7284 (1992).